# HALL CURRENT EFFECTS ON UNSTEADY MHD FLOW IN A ROTATING PARALLEL PLATE CHANNEL BOUNDED BY POROUS BED ON THE LOWER HALF – DARCY LAPWOOD MODEL

**L.HARI KRISHNA, M.VEERA KRISHNA ,M.C.RAJU**

**Abstract:** We studied the unsteady flow of a incompressible viscous fluid in a rotating parallel plate channel bounded on one side by a porous bed under the influence of a uniform transverse magnetic field taking hall current into account. The perturbations are created by a constant pressure gradient along the plates in addition to the non-torsional oscillations of the upper plate. The flow in the clean fluid region is governed by Navier-Stoke's equations while in the porous bed the equations are based on Darcy-Lapwood model. The exact solutions of the velocity in the clean fluid and the porous medium consist of steady state and transient state. The time required for the transient state to decay is evaluated in detail and ultimate quasi-steady state solution has been derived analytically, its behaviour computationally discussed with reference to the various governing parameters. The shear stresses on the boundaries and the mass flux are also obtained analytically and their behaviour is computationally discussed.

**Keywords:** Hall effects, MHD flows, Porous bed, unsteady flows and Rotating Parallel plate channels

**Introduction:** Flow of a viscous fluid in rotating channels is of considerable importance due to the occurrence of various natural phenomena and for its application in various technological situations which are governed by the action of Coriolis force. The broad subjects of oceanography, meteorology, atmospheric science and limnology all contain some important and essential features of rotating fluids. The viscous fluid flow problems in rotating medium under different conditions and configurations are investigated by many researchers in the past to analyze various aspects of the problem. The study of simultaneous effects of rotation and magnetic field on the fluid flow problems of a viscous incompressible electrically conducting fluid may find applications in the areas of geophysics, astrophysics and fluid engineering. An order of magnitude analysis shows that, in the basic field equations, the effects of Coriolis force are more significant as compared to that of inertial and viscous forces. Furthermore, it may be noted that Coriolis and magneto hydro dynamic forces are comparable in magnitude and Coriolis force induces secondary flow in the flow-field.

A large variety of processes of interest to industry and society involve the flow of fluids through porous media. Examples include the use of filtration to purify water and treat sewage, membranes to separate gases, the chemical reactors having porous catalysts supports. The mathematical modelling and simulation of the flow of fluids through porous media are important for designing and controlling a number of industrial processes including the production of fluids from underground reservoir and remediation of underground water resources. The simulation of flow is carried out using constitutive and conservative relations based on a macroscopic representation of porous media. There is a considerable interest in the recent years in the study of flow past a naturally permeable bed, with appropriate boundary conditions at a naturally permeable boundary. The usual conditions are, the normal flux is continuous and the tangential velocity is zero. The former is completely satisfactory but the latter is clearly only an approximation. As an alternative to these no-slip boundary conditions Beavers and Joseph [2] postulated, for the first time, the slip boundary condition which they had verified experimentally. The existence of the slip at the porous bed, due to the transfer of momentum from the free flow to Darcy flow which sets up the drag, is connected with presence of a very thin boundary layer of stream wise moving fluid just beneath the nominal surface of the permeable material. The fluid in this layer is pulled along by the flow in the channel.

Although the experiments were performed by Beavers and Joseph to test the validity of the proposed slip boundary conditions, owing to in adequate apparatus and instruments, the accuracy of experimental results was not sufficient to permit conclusive evaluation of the proposed analytical model although the existence of a slip velocity was confirmed qualitatively. Later experiments by Beavers, Sparrow and Magnuson [1], Rajasekhar *et.al* [5] investigated a steady laminar flow of forced convection through a channel having on porous bounding wall. They have taken into account the velocity slip at the surface of the porous medium and the contribution of heat due to viscous dissipation. Although the slip at the nominal surface was established based on the extension of a thin boundary layer just beneath the nominal surface attention was not focused on the analytical determination of the boundary layer thickness. Later Channabassappa and Ramanna [3] have determined analytically this boundary layer thickness. Rudraiah and Veerabhadraiah [6] have extended this analysis to include the buoyancy force. Rajasekhara [4] has performed the experiments to study the laminar flow characteristics in a composite channel considering Poiseuille flow, Couette flow and free surface flow. The aim of his experimental study was to determine the values of the slip parameter lower than that of Beavers & Joseph [2]. Such lower values are of importance in the design of porous bearings. Auxiliary experiments were also conducted to measure the values of k, the permeability of the porous medium. His experiments showed that for a particular porous materials namely natural sand $\alpha$ =0.01 as compared with $\alpha$ =0.1 of Beavers & Joseph [2] for foametal, and is independent of the depth of flow above bed. His experimental results were found to be in fair agreement with the analytical model which contains slip velocity at the permeable surface, except the mass flow rate which shows a slight deviation between experimental and theoretical data. Later Sasthry [7] studied the effect of the thickness of the porous lining on one side of the plate flow through a rotating parallel plate channel. And he discussed the flow in a rotating parallel plate channel with porous lining on both sides. In this paper, we discuss the unsteady flow of a incompressible viscous fluid in a rotating parallel plate channel bounded on one side by a porous bed under the influence of a uniform transverse magnetic field taking hall current into account.

**Formulation and solution of the problem:** We consider the unsteady flow of an in compressible viscous fluid in a rotating parallel plate channel bounded on one side by a porous bed subjected to a uniform transverse magnetic field normal to the channel. In the initial undisturbed state both the plates and the fluid rotate with the same angular velocity $\Omega$ . At $t$ >0 the fluid is driven by a constant pressure gradient parallel to the channel walls and in addition the upper plate perform non-torsional oscillations in its own plane.

We choose a Cartesian system O($x$, $y$, $z$) such that the boundary walls are at $z$=0 and $z$=$l$. $Z$-axis being the axis of rotation of the plates. The fluid medium consists of two zones namely zone 1and zone 2. Zone 1 consists of clean fluid governed by Navier-Stokes equations and zone 2 corresponds to the flow through porous bed governed by Darcy-Lapwood equations. At the interface the fluid satisfies the continuity condition of velocity and shear stress. The unsteady hydro magnetic equations governing the incompressible viscous fluid in zone 1 under the influence of transverse magnetic field with reference to a frame rotating with a constant angular velocity $\Omega$ are

$$\frac{\partial u}{\partial t} - 2\Omega\, v = -\frac{1}{\rho}\frac{\partial p}{\partial x} + \nu\frac{d^2u}{dz^2} + \mu_e J_y H_0 \tag{2.1}$$

$$\frac{\partial v}{\partial t} + 2\Omega\, u = -\frac{1}{\rho}\frac{\partial p}{\partial y} + \nu\frac{d^2v}{dz^2} - \mu_e J_x H_0 \tag{2.2}$$

The Darcy-Lapwood equations governing the flow through porous medium with respect to the rotating frame zone 2

$$\frac{1}{\delta}\frac{\partial u_p}{\partial t} - 2\Omega\, v_p = -\frac{1}{\rho}\frac{\partial p}{\partial x} - \frac{\nu}{k}u_p + \mu_e J_y^p H_0 \tag{2.3}$$

$$\frac{1}{\delta}\frac{\partial v_p}{\partial t}+2\Omega\, u_p \;=-\frac{1}{\rho}\frac{\partial p}{\partial y}-\frac{\nu}{k}v_p-\mu_e J_x^p H_0 \qquad (2.4)$$

Where $(u, v)$ and $(u_p, v_p)$ are velocity components along $O(x, y)$ directions respectively. $\rho$ the density of the fluid , $\sigma$ the conductivity of the medium, $\mu_e$ the magnetic permeability, $\nu$ the coefficient of kinematic viscosity, $\nu_{eff}$ the coefficient of effective kinematic viscosity, $k$ the permeability of the medium, $H_o$ is the applied magnetic field and $\delta$ is the porosity. Since the plates extends to infinity along $x$ and $y$ directions, all the physical quantities except the pressure depend on $z$ and $t$ alone. Hence $u$, $v$ and $u_p$, $v_p$ are function of $z$ and $t$ alone and hence the respective equations of continuity are trivially satisfied. When the strength of the magnetic field is very large, the generalized Ohm's law is modified to include the Hall current, so that

$$J+\frac{\omega_e\tau_e}{H_0}J\times H=\sigma\,(E+\mu_e\, q\times H) \qquad (2.5)$$

Where, q is the velocity vector, $H$ is the magnetic field intensity vector, $E$ is the electric field, $J$ is the current density vector, $\omega_e$ is the cyclotron frequency, $\tau_e$ is the electron collision time, $\sigma$ is the fluid conductivity and $\mu_e$ is the magnetic permeability. In equation (2.5) the electron pressure gradient, the ion-slip and thermo-electric effects are neglected. We also assume that the electric field $E$=0 under assumptions reduces to

$$J_x+m\;J_y=\sigma\mu_e H_0 v \qquad (2.6)$$

$$J_y-m\;J_x=-\sigma\mu_e H_0 u \qquad (2.7)$$

where $m=\omega_e\tau_e$ is the hall parameter.

On solving equations (2.6) and (2.7) we obtain

$$J_x=\frac{\sigma\mu_e H_0}{1+m^2}(v+mu) \qquad (2.8)$$

$$J_y=\frac{\sigma\mu_e H_0}{1+m^2}(mv-u) \qquad (2.9)$$

and similarly we obtain

$$J_x^p=\frac{\sigma\mu_e H_0}{1+m^2}(v+mu) \qquad (2.10)$$

$$J_y^p=\frac{\sigma\mu_e H_0}{1+m^2}(mv-u) \qquad (2.11)$$

Using the equations (2.8) and (2.9) the equations of the motion with reference to rotating frame zone 1 are given by

$$\frac{\partial u}{\partial t}-2\Omega\ v=-\frac{1}{\rho}\frac{\partial p}{\partial x}+\nu\frac{d^2u}{dz^2}+\frac{\sigma\mu_e^{\ 2}H_0^{\ 2}}{\rho(1+m^2)}(mv-u) \qquad (2.12)$$

$$\frac{\partial v}{\partial t}+2\Omega\ u\ =-\frac{1}{\rho}\frac{\partial p}{\partial y}+\nu\frac{d^2v}{dz^2}-\frac{\sigma\mu_e^{\ 2}H_0^{\ 2}}{\rho(1+m^2)}(v+mu) \qquad (2.13)$$

The Darcy-Lapwood equations governing the flow through porous medium with respect to the rotating frame zone 2 are given by

$$\frac{1}{\delta}\frac{\partial u_p}{\partial t}-2\Omega\ v_p=-\frac{1}{\rho}\frac{\partial p}{\partial x}-\frac{\nu}{k}u_p+\frac{\sigma\mu_e^{\ 2}H_0^{\ 2}}{\rho(1+m^2)}(mv_p-u_p) \qquad (2.14)$$

$$\frac{1}{\delta}\frac{\partial v_p}{\partial t}+2\Omega\ u_p\ =-\frac{1}{\rho}\frac{\partial p}{\partial y}-\frac{\nu}{k}v_p-\frac{\sigma\mu_e^{\ 2}H_0^{\ 2}}{\rho(1+m^2)}(v_p+mu_p) \qquad (2.15)$$

Let $q=u+iv$ , $\xi=x-iy$ , $q_p=u_p+iv_p$

Now combining equations (2.12) and (2.13), we obtain

$$\frac{\partial q}{\partial t}+2i\Omega\ q=-\frac{1}{\rho}\frac{\partial p}{\partial \xi}+\nu\frac{d^2q}{dz^2}+\frac{\sigma\mu_e^{\ 2}H_0^{\ 2}}{\rho(1+m^2)}(1+im)q \qquad (2.16)$$

and combining equations (2.14) and (2.15) , we obtain

$$\frac{1}{\delta}\frac{\partial q_p}{\partial t}+2i\Omega q_p=-\frac{1}{\rho}\frac{\partial p}{\partial \xi}-\frac{\sigma\mu_e^{\ 2}H_0^{\ 2}}{\rho(1+m^2)}(1+im)q_p-\frac{\nu}{k}q_p \qquad (2.17)$$

The boundary and initial conditions are

$$q\ =\ ae^{i\omega t}+be^{-i\omega t},\qquad z=l \qquad (2.18)$$

$$q_p=0,\quad t\neq 0,\qquad z=0 \qquad (2.19)$$

$$q\ =\ 0\ ,\quad q_p=\ 0,\ t=0\ ,\quad for\ all\ z \qquad (2.20)$$

At the interface we allow slip governed by Beaver-Joseph condition (Dimensional form)

$$\frac{\partial q}{\partial z}=\alpha D^{-1/2}(q_B-q_p)\qquad at\qquad z=h \qquad (2.21)$$

where $q_B$ is the slip velocity and $\alpha$ is the non-dimensional number (slip parameter). Also at the interface,

$$q=\ q_B\ ,\quad at\ \ z=h \qquad (2.22)$$

We introduce the following non dimensional variables are

$z^*=\frac{z}{l}$, $q^*=\frac{ql}{\nu}$ , $q^*_p=\frac{q_pl}{\nu}$ , $q^*_B=\frac{q_Bl}{\nu}$, $t^*=\frac{t\nu}{l^2}$, $\omega^*=\frac{\omega l^2}{\nu}$, $\xi^*=\frac{\xi}{l}$, $p^*=\frac{pl^2}{\rho\nu^2}$, $h^*=\frac{h}{l}$ Introducing these non-dimensional variables, the governing non-dimensional equations are (dropping the asterisks)

$$\frac{\partial q}{\partial t}+2iE^{-1}\ q=-\frac{\partial p}{\partial \xi}+\frac{\partial^2 q}{\partial z^2}-\frac{M^2(1+im)}{(1+m^2)}q \qquad (2.23)$$

$$\frac{1}{\delta}\frac{\partial q_p}{\partial t}+2iE^{-1}q_p=-\frac{\partial p}{\partial \xi}-\left(\frac{M^2(1+im)}{(1+m^2)}+D^{-1}\right)q_p \qquad (2.24)$$

Where,

$M^2=\dfrac{\sigma\mu_e^{\,2}H_0^{\,2}l^2}{\rho\nu}$ is the Hartmann number, $D^{-1}=\dfrac{l^2}{k}$ is the Inverse Darcy Parameter

$E=\dfrac{\nu}{\Omega l^2}$ is the Ekman number, $m=\omega_e\tau_e$ is the hall parameter, $P=\dfrac{\partial p}{\partial \xi}$ is the applied pressure gradient

The corresponding non-dimensional boundary and initial conditions are

$$q = ae^{i\omega t}+be^{-i\omega t}, \qquad z=1 \qquad (2.25)$$

$$q_p = 0, \qquad t\neq 0, \qquad z=0 \qquad (2.26)$$

$$q = 0, \quad q_p = 0, \; t\leq 0, \; for\ all\ z \qquad (2.27)$$

The Beaver-Joseph condition reduces to

$$\frac{\partial q}{\partial z}=\alpha D^{-1/2}(q_B-q_p), \qquad z=h \qquad (2.28)$$

The interfacial condition is

$$q = q_B \qquad , z=h \qquad (2.29)$$

Taking Laplace transforms of equations (2.23) and (2.24) using initial condition (2.26) to (2.27). We obtained the solutions *q* and $q_B$.

The shear stresses on the upper plate and lower plate are given by

$$\tau_U=\left(\frac{dq}{dz}\right)_{z=1} \quad \text{and} \quad \tau_L=\left(\frac{dq}{dz}\right)_{z=h}$$

We also determine the mass flux by the formula,

$$Q_x+iQ_y=\int_h^1 q\,dz, \;\; i.e., Mass\ \ flux=Q=\sqrt{Q_x^{\,2}+Q_y^{\,2}}$$

**Results and Discussion**: The slip velocity $q_B$ has been calculated using B-J condition (2.33) and is governed by the expression (2.44). The velocity profiles for *u* and *v* in the clean fluid region have been drawn figures (1-8) for the variations in the governing parameters and fixing the other parameters ( $a=1,\ b=1,\ \delta=0.3,\alpha=0.5,\beta=1.2,\ \omega=\pi/4$). We notice that *u* enhances with *E* or *m* and reduces with *M* or $D^{-1}$ in either case of smaller and larger thickness of porous bed (fig 1-8). The resultant velocity however enhances with *E* and *m* and reduces with *M* and $D^{-1}$ irrespective of the thickness of the porous bed and is always directed away from the central axis of the channel with phase difference greater than $7\pi/4$ from the direction of the imposed pressure gradient tabulated. The slip velocities $u_B$ and $v_B$ have been calculated at tabulated in the tables (1 and 2) for the different variations in the governing parameters. The slip velocity $u_B$ enhances with its magnitude with increasing in *E*, *m*, *M* and $D^{-1}$ for the smaller and larger thickness of porous bed (Table 1). The slip velocity $v_B$ enhances with its magnitude increase in *E* or *m* while reduces with increases in *M* (or) $D^{-1}$ for the irrespective thickness of porous bed (Table 2). The shear stresses of the upper and lower plate are evaluated and tabulated in tables (3-6). Table (3) indicates $\tau_x$ for variations in the governing parameters in case of smaller and larger thickness of the porous bed. The table 4 represents to these variations for $\tau_y$ for the upper plate. We find that $\tau_x$ and $\tau_y$ reduces with E or *m* irrespective of thickness (0.2 & 0.5), and an increasing in *M* or $D^{-1}$ enhances $\tau_x$ and $\tau_y$ reduces irrespective of thickness (0.2 & 0.5).

**Graphs and Tables:**

I. **Velocity Profiles for *u* & *v* when the thickness of the porous bed (h=0.2) is small**

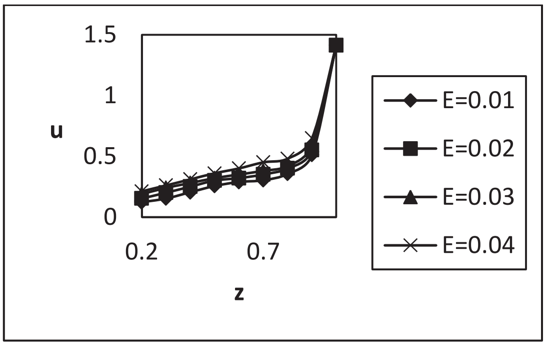


Figure 1. The velocity profile for *u* against *E* with $M=2, D^{-1}=1000, m=1$

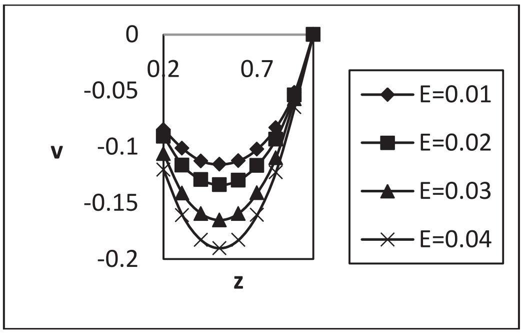


Figure 2. The velocity profile for *v* against *E* with $M=2, D^{-1}=1000, m=1$

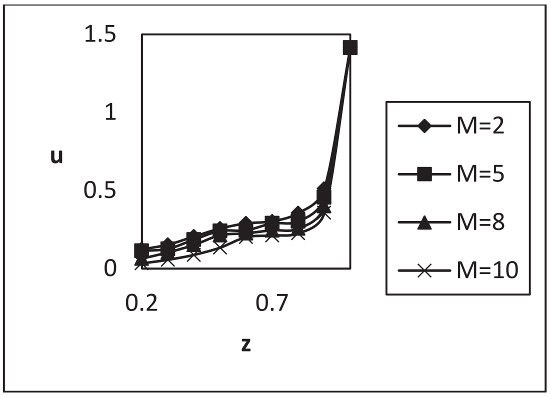


Figure 3. The velocity profile for *u* against *M* with $E = 0.01, D^{-1} = 1000, m = 1$

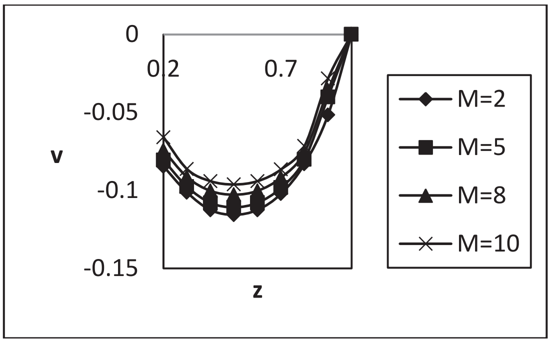


Figure 4. The velocity profile for *v* against *M* with $E = 0.01, D^{-1} = 1000, m = 1$

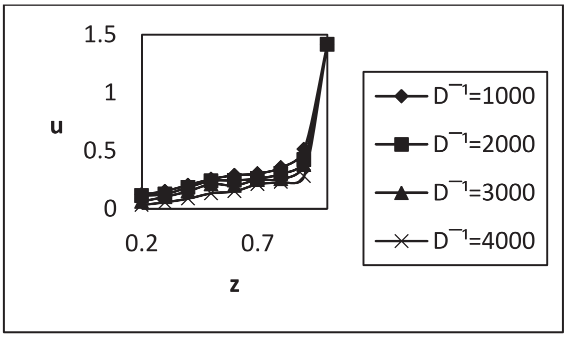


Figure 5. The velocity profile for *u* against $D^{-1}$ with $E = 0.01, M = 2, m = 1$

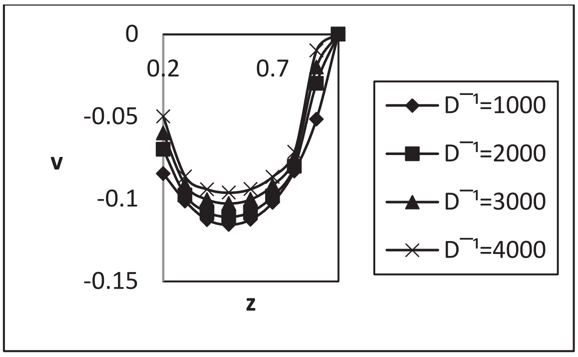


Figure 6. The velocity profile for *v* against $D^{-1}$ with $E = 0.01, M = 2, m = 1$

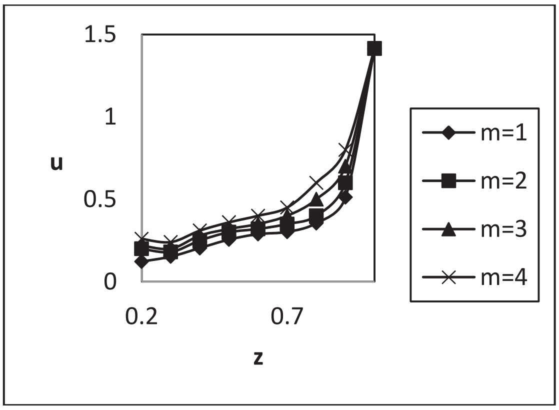


Figure 7. The velocity profile for *u* against *m* with $E = 0.01, M = 2, D^{-1} = 1000$

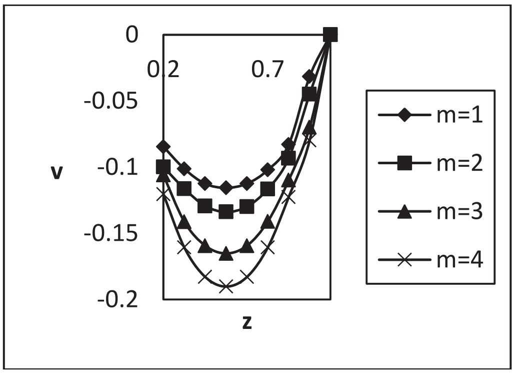


Figure 8. The velocity profile for *v* against *m* with $E = 0.01, M = 2, D^{-1} = 1000$

| h | I | II | III | IV | V | VI | VII | VIII | IX |
|---|---|---|---|---|---|---|---|---|---|
| 0.2 | 0.12252 | 0.15228 | 0.18856 | 0.1133 | 0.0633 | 0.1245 | 0.0688 | 0.2002 | 0.2265 |
| 0.5 | 0.28554 | 0.33225 | 0.38856 | 0.2402 | 0.2125 | 0.2568 | 0.2245 | 0.3522 | 0.4526 |

| | I | II | III | IV | V | VI | VII | VIII | IX |
|---|---|---|---|---|---|---|---|---|---|

| | | | | | | | | | |
|---|---|---|---|---|---|---|---|---|---|
| $E$ | 0.01 | 0.02 | 0.03 | 0.01 | 0.01 | 0.01 | 0.01 | 0.01 | 0.01 |
| $M$ | 2 | 2 | 2 | 5 | 8 | 2 | 2 | 2 | 2 |
| $D^{-1}$ | 1000 | 1000 | 1000 | 1000 | 1000 | 2000 | 3000 | 1000 | 1000 |
| $m$ | 1 | 1 | 1 | 1 | 1 | 1 | 1 | 2 | 3 |

Table 1. The slip velocity $u_B$

| h | I | II | III | IV | V | VI | VII | VIII | IX |
|---|---|---|---|---|---|---|---|---|---|
| 0.2 | -0.084 | -0.0912 | -0.1065 | -0.0811 | -0.074 | -0.072 | -0.065 | -0.1022 | -0.1062 |
| 0.5 | -0.1156 | -0.1339 | -0.1652 | -0.1109 | -0.1028 | -0.1058 | -0.1025 | -0.1339 | -0.1652 |

| | I | II | III | IV | V | VI | VII | VIII | IX |
|---|---|---|---|---|---|---|---|---|---|
| $E$ | 0.01 | 0.02 | 0.03 | 0.01 | 0.01 | 0.01 | 0.01 | 0.01 | 0.01 |
| $M$ | 2 | 2 | 2 | 5 | 8 | 2 | 2 | 2 | 2 |
| $D^{-1}$ | 1000 | 1000 | 1000 | 1000 | 1000 | 2000 | 3000 | 1000 | 1000 |
| $m$ | 1 | 1 | 1 | 1 | 1 | 1 | 1 | 2 | 3 |

Table 2. The slip velocity $v_B$

| h | I | II | III | IV | V | VI | VII | VIII | IX |
|---|---|---|---|---|---|---|---|---|---|
| 0.2 | 2.49444 | 1.49775 | 0.77973 | 3.96435 | 4.38864 | 3.54346 | 5.71434 | 1.25563 | 1.02256 |
| 0.5 | 2.49512 | 1.58992 | 0.79145 | 3.45126 | 4.12855 | 3.57835 | 5.82945 | 1.28596 | 1.05266 |

| | I | II | III | IV | V | VI | VII | VIII | IX |
|---|---|---|---|---|---|---|---|---|---|
| $E$ | 0.01 | 0.02 | 0.03 | 0.01 | 0.01 | 0.01 | 0.01 | 0.01 | 0.01 |
| $M$ | 2 | 2 | 2 | 5 | 8 | 2 | 2 | 2 | 2 |
| $D^{-1}$ | 1000 | 1000 | 1000 | 1000 | 1000 | 2000 | 3000 | 1000 | 1000 |
| $m$ | 1 | 1 | 1 | 1 | 1 | 1 | 1 | 2 | 3 |

Table 3. The shear stress $(\tau_x)$ on the upper plate.

| h | I | II | III | IV | V | VI | VII | VIII | IX |
|---|---|---|---|---|---|---|---|---|---|
| 0.2 | -0.5224 | -0.4209 | -0.3665 | -0.6985 | -0.7854 | -0.8544 | -1.2232 | -0.3556 | -0.1445 |
| 0.5 | -0.6878 | -0.5988 | -0.4874 | -0.7488 | -0.8556 | -9.2565 | -2.0013 | -0.4745 | -0.3568 |

| | I | II | III | IV | V | VI | VII | VIII | IX |
|---|---|---|---|---|---|---|---|---|---|
| $E$ | 0.01 | 0.02 | 0.03 | 0.01 | 0.01 | 0.01 | 0.01 | 0.01 | 0.01 |
| $M$ | 2 | 2 | 2 | 5 | 8 | 2 | 2 | 2 | 2 |
| $D^{-1}$ | 1000 | 1000 | 1000 | 1000 | 1000 | 2000 | 3000 | 1000 | 1000 |
| $m$ | 1 | 1 | 1 | 1 | 1 | 1 | 1 | 2 | 3 |

Table 4. The shear stress $(\tau_y)$ on the upper plate.

**Conclusions:**

1. The slip velocity $q_B$ has been calculated using B-J condition. The slip velocity $u_B$ enhances with its magnitude with increasing in $E$, $M$ and $D^{-1}$ for the smaller and larger thickness of porous bed. The slip velocity $v_B$ enhances with its magnitude increase in $E$ or $m$ while reduces with increases in $M$ (or) $D^{-1}$ for the irrespective thickness of porous bed.
2. The magnitude of the velocity component $u$ enhances with $E$ or $m$ and reduces with $M$ or $D^{-1}$ in either case of smaller and larger thickness of porous bed.
3. The magnitude of the velocity component $v$ enhances with $E$ but reduces with $M$, $m$ and $D^{-1}$ in either cases of smaller and larger thickness of porous bed.
4. The resultant velocity however enhances with $E$ and $m$ and reduces with $M$ and $D^{-1}$ irrespective of the thickness of the porous bed and is always directed away from the central axis of the channel with phase difference greater than $7\pi/4$ from the direction of the imposed pressure gradient.

**References:**


1. Beavers,G.S. Sparrow,E.V. & Hagnuson,R.A. *Trans.ASME.J.Basic Engg.* vol. 92 (1970).p-843.
2. N.Vithya, Dr. P. Thangavelu, on Generalised B#- Closed Sets; Mathematical Sciences international Research Journal ISSN 2278 – 8697 Vol 3 Issue 2 (2014), Pg 561-563
3. Beavers,G.s. & Joseph,D.D. *Jour.Flu.Mech.*vol.30 (1967),p-197.
4. Channabassappa & Ramanna. *Appl.sci.res.*vol. 32 (1976).
5. Rajashekara,B.M. Ph.D. Thesis, Experimental and theoretical study of flow past a porous medium. Banglore University (1974).
6. Rajashekara,B.M.Ramaiah, B.K. & Rudraiah,N. *Current Scence*,vol-40,issue-21 (1971), p-561.
7. S. Sudha,K. Manikandan, total Coloring and (***K, D***)- total Coloring of Prisms; Mathematical Sciences International Research Journal ISSN 2278 – 8697 Vol 3 Issue 1 (2014), Pg 11-13
8. Rudraiah & Veerabhadraiah, *Proc. Indian Acad.Sci.A.* vol. 86 (1975,1977), p. 537.
9. Sasthry.D.R.V.S.R.K. "Flow in a Rotating parallel plate channel with porous lining" *M.Phil.Thesis*, Andhra University, Vishakhapatnam (2005).


Dept of Mathematics, Annamacharya Institute of Technology and Science, Rajampet, Kadapa,Andhra Pradesh, India, Email: lhkmaths@gmail.com
Dept of Mathematics, Rayalaseema University, Kurnool, AP, India
Dept of Mathematics, Annamacharya Institute of Technology and Science, Rajampet, Kadapa, Andhra Pradesh, India